JOURNAL OF AIRCRAFT
Vol. 32, No. 3, May–June 1995

Statistical Discrete Gust–Power Spectral Density Methods Overlap—Holistic Proof and Beyond

Robert P. Chen*
Allied-Signal Aerospace Company, Torrance, California 90504-6061

The statistical discrete gust (SDG)–power spectral density overlap of $\bar{\gamma} = 10.4\bar{A}$ claimed by J. G. Jones, and verified by B. Perry III, A. S. Pototzky, and J. A. Woods, does exist. The analytical results consist of numerical substantiation of specific aircraft models. The claim is valid up to approximately ±10% about the 10.4 factor. This article presents a mathematically rigorous proof from basic principles without specific aircraft models and very restricted gust shapes. By invoking Chebyshev's inequality, the extension to $\bar{\gamma}_{max} = 25–150\bar{A}$ for true design gust loads becomes a reality to complete the holistic proof. This article also introduces the all-encompassing fractal geometry representation of turbulence that uses their respective Hausdorff (fractal) dimensions to derive all known spectral shapes. A sample case explains the obvious impacts from these different shapes on gust load exceedance. A two-tier approach proposes concrete changes in FAR 25 requirements. Realistic assessment of SDG method's role in gust load analysis points out some of its shortcomings and virtues.

Introduction

THIS article presents a rigorous proof from basic principles and established values of rms gust velocity, the hitherto unfamiliar claim by Jones[1] that $\bar{\gamma} = 10.4\bar{A}$, where $\bar{\gamma}$ = maximum value of worst case responses for different combinations of ramp-hold gusts in the statistical discrete gust (SDG) method, and $\bar{A}$ = the ratio of rms output to rms input of the power spectral density (PSD) method. Although Perry et al.[2] have verified numerically its validity, this claim alone does not allow the SDG method to become a stand-alone or alternate candidate for gust loads determination. By invoking Chebyshev's inequality, a set of multiplier values >10.4 becomes available from either Gaussian or non-Gaussian distribution. These values, in the range of 25–150, have the same order of magnitude as the U_σ prescribed by FAR 25 and JAR 25. They can be the design limit and ultimate load requirements without any reservation.

The often quoted, but rarely verified fact that fractal representations of turbulence, self-similarity, self-affinity, intermittency[3,4]. . . $k = 1/3$, similarity parameter, will inevitably lead to von Kármán spectrum with a $-5/3$ slope[5,6] is proved from fractal dimension considerations[7] and Fourier transforms due to Lighthill.[8] A three-vortex-sheets model extracted from a 3 × 3 × 3 cube furnishes a unified approach in deriving the well-known Dryden spectrum with a -2 slope, the somewhat obscure modified Lappe spectrum with a -1.8 slope,[9] the aforementioned von Kármán spectrum with a $-5/3$ slope, and all other power law slopes.

A historical sample from Lockheed-Georgia company's C-5A Galaxy[9,10] demonstrates the pitfalls of employing modified Lappe spectrum for both nonstorm and storm parts of exceedance. A one-segment mission analysis effectively pinpoints the unconservative middle exceedance, medium load level zone for the C-5A. This shortage in exceedance is most probably the root-cause for not meeting design service life. In using the von Kármán spectrum for both nonstorm and storm parts of exceedance, the overconservatism clearly shows at low exceedance, high load level zone. The proposed FAR 25 requirements' change to reduced slopes directs toward this end of the exceedance.[11]

Realistic assessment of SDG method's role in gust loads determination furnishes some overall conclusions and recommendations on wider issues such as the feasibility of extending the fractal/wavelet transforms[12] representations to gust responses (i.e., random outputs). If this approach is possible, a new counterpart of the PSD method's transfer function[13] will be readily realized for an improved SDG method. Although the SDG method has had most attention in the United Kingdom,[14,15] improved SDG methods should enable a wider acceptance.

Proof of Overlap and Its Extension

The SDG–PSD overlap claimed by Jones,[1] and verified by Perry et al.[2] does exist. The former claims $\bar{\gamma} = 10.4\bar{A}$, and the latter shows $\bar{\gamma} = 9.51–11.13\bar{A}$ for rigid body and 8.49–11.50$\bar{A}$ for fully flexible models, respectively. A proof with mathematical rigor has the following steps:

$$\begin{aligned}\bar{\gamma} &= \max x \approx E[3\sigma_x] = 3E[(\sigma_x/\sigma_w)\sigma_w] \\ &= 3E[\sigma_x/\sigma_w]E[\sigma_w] = 3\bar{A}b_1\end{aligned} \tag{1}$$

The first equality $\bar{\gamma} = \max x$, and the last equality $E[\sigma_x/\sigma_w] = \bar{A}$ are the very definitions of $\bar{\gamma}$ and $\bar{A}$, respectively. The approximation $\max x \approx 3\sigma_x$ is a well-accepted assumption for a Gaussian distribution. $E[kx] = kE[x]$, $E[xy] = E[x]E[y]$ are in most probability and mathematical statistics' text books.[16] Houbolt[17,18] and FAR 25[19] give $E[\sigma_w] = b_1 \equiv 3$ ft/s. Wang and Shen[20] give the non-Gaussian distributed version of Eq. (1):

$$\bar{\gamma}_{ng} = \max x \approx E[3.5\sigma_x] = 3.5\bar{A}b_1 \tag{2}$$

Thus, $\bar{\gamma} = 9\bar{A}$ to $10.5\bar{A}$; or $\bar{\gamma} \approx 10.4\bar{A}$ is admissible to be true. Incidentally, Etkin[21] and Hoblit[22] define U_σ along similar thoughts

$$x_{design} = \eta_d\sigma_x = \eta_d\sigma_w(\sigma_x/\sigma_w) = U_\sigma\bar{A} \tag{3}$$

where η_d = design ratio of peak to rms value for x, and $U_\sigma = \eta_d\sigma_w$ = design gust velocity.

The thwarted linking of $x_{design} = \bar{\gamma} = 10.4\bar{A} = U_\sigma\bar{A}$ with $U_\sigma = \eta_d\sigma_w = \eta_d b_i = 10.4$, $i = 1, 2$; is the mediocre $\eta_d \sim 3.5$, $b_1 = 3$; and $\eta_d \sim 0.87$, $b_2 = 12$ combinations that def-

Received March 7, 1994; presented as Paper 94-1724 at the Dynamic Specialist Conference, Hilton Head, SC, April 21–22, 1994; revision received Sept. 11, 1994; accepted for publication Sept. 13, 1994.

*Engineering Specialist, Aerospace Systems and Equipment, Engineering Sciences. Member AIAA.

initely seem to be lacking in magnitude by intuition. Moreover, by invoking the lower bound values of Chebyshev's inequality[23]

$$P(|x - m| \leq h\sigma) = \int_{m-h\sigma}^{m+h\sigma} p(x)\,dx \geq 1 - 1/h^2 \quad (4)$$

Much larger (than η_d) h values are available. Figure 1 shows the P for three distributions and the logic to obtain h (lower bound) values from $P(|x| \leq h\sigma) = Q(h) = 1 - 1/h^2$.

Therefore, $h = 3$ for $P(|x| \leq 3\sigma_x) = 0.9974$ with $p(x)$ Gaussian, or $0.9974 \geq 1 - 1/h^2$, which gives $h^2 \leq 1/0.0026$, and $h \leq \sqrt{1/0.0026} = 19.6116$. Let $\bar{y}_{max} = h\sigma_x = h\bar{A}b_1 = 19.6116\bar{A}3.0 = 58.8348\bar{A} \approx 59\bar{A}$. Similarly, $h = 3.5$ for a non-Gaussian distribution[20] gives $P(|x| \leq 3.5\sigma_x) = 0.9996$, or $h_{ng} \leq \sqrt{1/0.0004} = 50$. This gives $\bar{y}_{max\,ng} = h_{ng}\bar{A}b_1 = 50\bar{A}3.0 = 150\bar{A}$.

It is interesting to recall that FAR 25 Appendix G requires $x_{limit} = U_\sigma\bar{A} = 25$–$85\bar{A}$ for cruise at various altitudes. The corresponding U_σ for gust penetration and dive are 132 and 50% of the above, respectively. If one assumes $x_{limit} \sim \bar{y}_{max}$ or $\bar{y}_{max\,ng}$, the order of magnitude for U_σ is the same as 59–150. Hence, the recommended values of U_σ in FAR 25 are acceptable. Moreover, $\bar{y}_{max}$ or $\bar{y}_{max\,ng} \neq \bar{y}$, and $>10.4\bar{A}$. With the values of $\bar{y} = 9$–$10.5\bar{A}$, for a Gaussian or non-Gaussian process, established from $b_1 \equiv 3$ ft/s, and $\bar{y} = 3\sigma_x$ or $3.5\sigma_x$, the holistic proofs for the SDG-PSD overlap à la Jones is at hand.

Ramifications Beyond Overlap and Their Effects on Design Gust Velocity

The beyond part starts with the $\bar{y}_{max} = 59$–$150\bar{A}$ from Chebyshev's inequality, for $h = 19.6116$ and $h_{ng} = 50$. It is obvious that 59 and 150 are quantities proportional to U_{de} or U_σ in the FAR 25 requirements. They are exactly the post $\bar{y} = 10.4\bar{A}$, nonoverlapped areas in the Venn diagram that Perry et al. have suggested in their reply[14] to Etkin's comment.[15] Although they are larger than the FAR 25 U_σ values, the discrepancy is inherent in Chebyshev's inequality being the absolute lower bound (see Fig. 1).

More relaxed lower bounds do exist if the third and fourth moments of x are available. The former is a measure of skewness and the latter is a measure of flatness. Lin[24] showed that nonlinear stress responses with negative peaks have a positively skewed Rayleigh or modified Rayleigh distribution. Wang and Shen,[20] and Chen[25] reported non-Gaussian, large flatness factor, gust velocity distributions sometime ago.

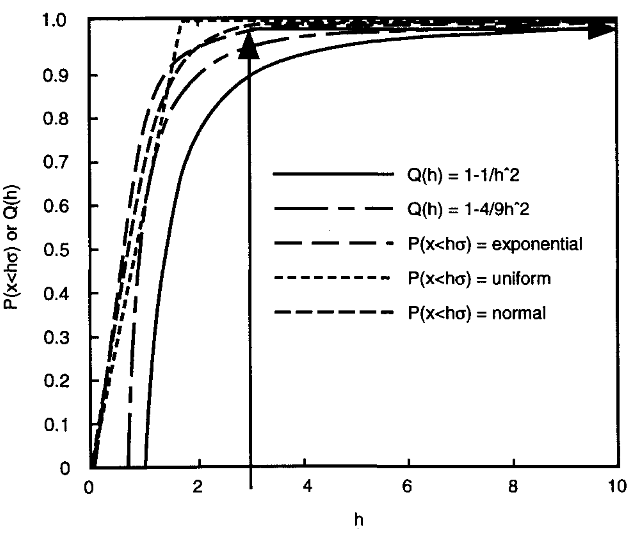

Fig. 1 Graphs of three distributions and two lower bounds.

H. Cramèr[26] has cast the Chebyshev inequality in the Bienaymé-Chebyshev form:

$$P(|\xi - m| \geq k\sigma) \leq l/k^2 \quad (5)$$

He also gives a number of more relaxed forms for non-Gaussian distributions:

1) For a skewed distribution, a Gauss unimodal correction is available:

$$P(|\xi - x_0| \geq k\tau) \leq 4/9k^2 \quad (6)$$

where x_0 = mode of x, m = mean of x, and $\tau^2 = \sigma^2 + (x_0 - m)^2$. A heuristic approximation is readily realizable if $x_0 \to m$, or $|x_0 - m| << \sigma$, then $\tau^2 \approx \sigma^2$ and

$$1/h^2 = 4/9k^2 \qquad \text{or} \qquad k = 2h/3 \quad (7)$$

Equation (7) simply says that, for a skewed distribution, the effective h value k, is $\frac{2}{3}h$, where h is the number of σ in Eq. (4).

2) For a skewed and nonflat (flatness factor >3) distribution with both third and fourth moments (i.e., μ_3 and μ_4) available

$$P(|\xi - m| \geq k\sigma) \leq 4(1 + s^2)/9(k - |s|)^2 \quad (8)$$

where s is the Pearson measure of skewness and flatness as defined in the following:

$$s = (m - x_0)/\sigma = \gamma_1(\gamma_2 + 6)/2(5\gamma_2 - 6\gamma_1^2 + 6) \leq 0.25 \quad (9)$$

$$\gamma_1 = \mu_3/\sigma^3 \quad (10a)$$

$$\gamma_2 = \mu_4/\sigma^4 - 3 = \text{flatness factor} - 3 \quad (10b)$$

References 20 and 25 have the flatness factor values for some measured vertical gust velocity distributions. They are, flatness factor = 3–3.51. No published γ_1 value is available, except $s \leq 0.25$. γ_1 uses a series of realistic values to check its effect on k with $\sigma_w = b_1 \equiv 3$ ft/s. Table 1 lists the results of this comparison together with some approximations from Eq. (8) for $s^2 \to 0$; s, γ_1, $\gamma_2 \neq 0$. Clearly, once the skewness is nonzero, $k \approx \frac{2}{3}h$ is a good approximation for any γ_1, γ_2, or s corrections. The best result comes from $\gamma_1 = 0.50$ and $\gamma_2 = 0$ to 0.51; furthermore, the skewness requirement is quite easy to fulfill, if one recalls the following:

1) A narrow-band Gaussian process' peak distribution is Rayleigh.

2) A collection of mostly nonoverlapping Gaussian distributed time histories would have a skewed joint probability density function, if one non-Gaussian distributed time history were included.

With these two facts, $\bar{y} \approx 10.4\bar{A}$ and $\bar{y}_{max} = 25$–$150\bar{A}$, established from a mathematical rigorous and probabilistic sound basis; the proof of overlap requires no other corroboration. Nevertheless, in establishing the validity of the $U_\sigma = 25$–150 values, a useful U_{de}/U_σ vs altitude plot with isoprobability lines becomes evident as a byproduct from the VG, VGH, and extreme-value theory approach.[27–29] The ramifications are as follows:

1) The U_σ values 10.4, 25, 42, 59, and 150 at the top of Figs. 2a and 2b illustrate their credibility. Obviously, the 10.4 value is too low with a $P(U_{de} \geq 10.4) = 1 \times 10^{-2}$, or as an exceedance of once per 100 flight hours. The corresponding $P(U_\sigma \geq 19) = 1 \times 10^{-2}$ is slightly higher for U_σ, but still low in flight hours.

2) The range of $U_\sigma = 25$–59 corresponds to $P(U_{de} \geq 25) = 2 \times 10^{-4}$ at 70,000 ft and $P(U_{de} \geq 59) = 5 \times 10^{-7}$ at 50,000 ft, respectively. The exceedances are once per 5000 flight hours and once per $2 \times 10^{+6}$ flight hours, respectively, from Fig. 2b. They fit the design envelope floor for use with mission analysis from 31,000 to 80,000 ft as shown in Fig. 2a.

Table 1 Comparison of various design gust velocities U_σ at different lower bounds

Type of inequality, h	Bienaymé-Chebyshev, Eq. (5): $k = h$	Bienaymé-Chebyshev, Eq. (5): $U_\sigma = k\sigma^a$	Skewed Gauss unimodal correction, Eq. (6): $k = 2/3h$	Skewed Gauss unimodal correction, Eq. (6): $U_\sigma = k\sigma$	Pearson measure of skewness and flatness, Eq. (8): $k^b = 2/3h + s$	$U_\sigma = k\sigma$	$k^b = 2/3h \sqrt{(1 + s^2)} + s$	$U_\sigma = k\sigma$	$k^c = 2/3h \sqrt{(1 + s^2)} + s$	$U_\sigma = k\sigma$
Gaussian 3.0	3.0	9.0	2.0	6.0	2.025	6.075	2.0256	6.0769	2.2835	6.8506
					2.25	6.75	2.3116	6.9347	2.4415	7.3246
Non-Gaussian	3.5	10.5	7/3	7.0	2.3583	7.075	2.3591	7.0772	2.6256	7.8769
3.5					2.5833	7.75	2.6551	7.9654	2.7929	8.3786
Gaussian $Q(h)$	19.6116	58.8348	4.6829	14.0488	4.8337	14.5010	4.8337	14.5010	6.6815	20.0446
19.6116					6.4108	19.2055	7.1429	21.4286	8.2761	24.8282
Non-Gaussian	50.0	150.0	7.1429	21.4286	7.4125	22.2375	7.4125	22.2375	10.7211	32.1634
$Q(h)$ 50.0					10.1015	30.3046	11.4708	34.4124	13.8675	41.6025

[a] $\sigma = b_1 = 3$ ft/s. [b] $s = 0.025$ and 0.25, and $s^2 \rightarrow 0$ in column 6. [c] $s = 0.2309$ and 0.3333, for $\gamma_1 = 2s = 0.50$ and $\gamma_2 = 0$–0.51 from flatness factor 3.0 to 3.51, and Eqs. (9), (10a), and (10b).

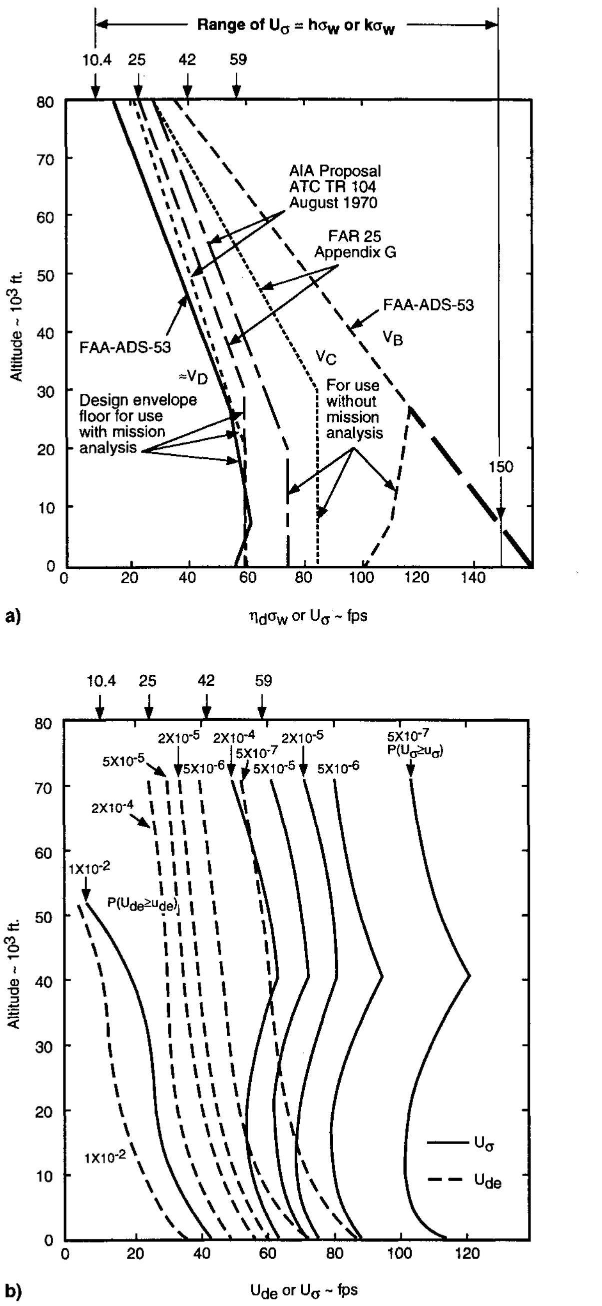

Fig. 2 a) Various proposals for U_σ with altitude and b) isoprobability levels for U_{de} and U_σ with altitude.

3) Similarly, for U_σ = 42–150; the values fit the FAA-ADS-53 recommended max U_σ line for use without mission analysis from 6000 to 77,000 ft. The 27,000-ft corner extrapolates to 6000 ft for U_σ = 150 (see Fig. 2a). For the same $P(U_\sigma \geq u_\sigma) = 2 \times 10^{-4}$ at 70,000 ft, 5×10^{-6} at 60,000 ft, and 5×10^{-7} at 50,000 ft; the U_σ are 53, 84, and 113 ft/s, respectively (see Fig. 2b).

The validity of the relaxed (and standard) Chebyshev inequality derived U_σ is unquestionable with various proposed values shown in Fig. 2a, taken from Ref. 22, Fig. 5.5. The sources quoted therein (i.e., FAA-ADS-53, FAR 25 Appendix G, AIA proposal ATC TR104) are the current norm. This "beyond" byproduct permits a rational probability based selection of U_{de}/U_σ for V_C (V_B and V_D), with expected quantitative gust encounter frequencies included (e.g., once per 50,000 flight hours = $P = 2 \times 10^{-5}$). This last feature incorporates easily into the current FAR 25 requirements for future transport aircraft gust load optimization.

Fractal Geometry Representation of Turbulence

Using the Jones[1] implied, fractal related $k = 1/3$, leading to von Kármán spectrum with a slope of $-5/3$, and observations beyond Mandelbrot,[7] one can demonstrate the versatility of a three-vortex-sheets cube. Table 2 depicts the five turbulence models in ascending order of severity. Following the rows in Table 2, they are as follows: 1) a single vortex sheet (two-dimensional); 2) a set of three layered vortex sheets taken out of a three-dimensional cube; 3) one folded up and down side squares middle sheet, with top and bottom Sierpinski carpets[7]; 4) a hydrant[30] formed by a break-away top sheet; and 5) a modified hydrant with partially broken, fully closed (by a 60-deg pyramid) top tube.

The fractal dimension D defined by Mandelbrot has the following expression:

$$D = \log N/\log 1/r \tag{11}$$

where N = number of basic units (squares) in the assembly, r = ratio of measuring unit to original length of side, ($r < 1$ or $1/r > 1$ always). The columns, with the headings E, D, and D_T, list the values for the five models. The letters E, D, and D_T are Euclidean, fractal, and topological dimensions, respectively. Table 2 also tabulates the similarity parameter k with three different expressions.[7,12,31]

Clearly, the first model is a two-dimensional plane, therefore, $E = D_T = 2$. Moreover, it consists of nine small squares with their sides' one, or $N = 9$ and $r = 1/3$ that gives $D = \log 9/\log 3 = 2$. The second to fifth models are either three or two (two-dimensional) sheets stacked to a finite (one-dimensional) height or one (two-dimensional) bottom sheet with a finite (one-dimensional) height for the center tube; hence, $E = 3$. The sheets and the center tube form a connected

Table 2 Five turbulence models derived from a three-vortex sheets cube

Turbulence type	Model/ intersection	Dimension			Similarity parameter, k			Power for variance of turbulent velocity		Power for spectrum at $\omega >> \omega_{knee}$	Known spectra with same power
		E	D	D_T	$1/D$	$D - 2/3$	$5 - D/6$	$B = 3 - D/3$	$\alpha = 2/3 + B$	$-(\alpha + 1)$	
Normal, nonstorm	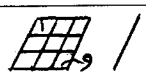	2	2	2	0.5	0	0.5	1/3	1	−2	Dryden, Lappe
		3	3	2	1/3	1/3	1/3	0	2/3	−5/3	von Kármán
Transition	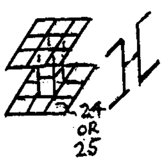	3 3	2.9299 2.8928	2 2	0.3413 0.3457	0.3099 0.2976	0.3450 0.3512	0.0234 0.0357	0.6901 0.7024	−1.6901 −1.7024	
Severe, storm	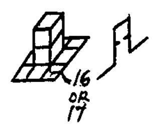	3 3	2.5789 2.5237	2 2	0.3878 0.3962	0.1929 0.1745	0.4035 0.4127	0.1404 0.1588	0.8071 0.8255	−1.8071 −1.8255	Modified Lappe[9] Burns[32]
	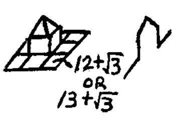	3 3	2.4486 2.3846	2 2	0.4084 0.4196	0.1495 0.1282	0.4252 0.4359	0.1838 0.2051	0.8505 0.8718	−1.8505 −1.8718	

surface; therefore, $D_T = 2$. Table 2 lists the D for all cases computed from Eq. (11) by counting N squares in the assembly and $1/r = 3$.

A word of caution for rows 3–5, the top and bottom sheets are always Sierpinski carpets[7] with their center squares removed. The middle sheet can be either a full nine squares or an eight-square Sierpinski carpet. The reasons for keeping the center square for the middle sheet are threefold:

1) It is the base to fold the middle sheet into a tube with four cuts.

2) Its presence helps the tube from premature collapse when the top sheet breaks away.

3) The added mass of the center square will aid in forming the four equilateral triangles for the last case. Albeit the conjectures are the author's, they are at least strongly consistent if not necessarily true in view of the B values, obtained from 17 squares and 12 squares plus 4 equilateral triangles, and fit Chorin's $B = 0.17 \pm 0.03$.[7]

Insofar as how these insights came up, suffice it to say that slight modifications of the fourth and fifth models give $N = 17 + \sqrt{3}$ and $14 + \sqrt{3}$, or $D = 8/3$ and $5/2$, respectively, they are exactly the fractal dimensions for the classic Kolmogorov and Burgers turbulence models. Also, the third and fourth models are mere extensions of Rucker's hydrant[30] that is nothing more than the Sierpinski carpet plus a center cube.

Unified Theory for Various Known Spectral Shapes

Another apposite feature of fractal geometry representation for turbulence is its unified approach. Instead of citing the well-known Wiener-Khintchine relationship for autocorrelation function and power spectral density; one uses directly the Fourier transform of $|x|^\alpha$ as introduced by Lighthill,[8] Mandelbrot's variance of turbulent velocity definition of $\langle |V(x) - V(x + r)|^2\rangle = |r|^{2/3+B}$, and $B = 3 - D/3$. The slope for $\omega >> \omega_{knee}$ established for Dryden spectrum ($D = 2$), von

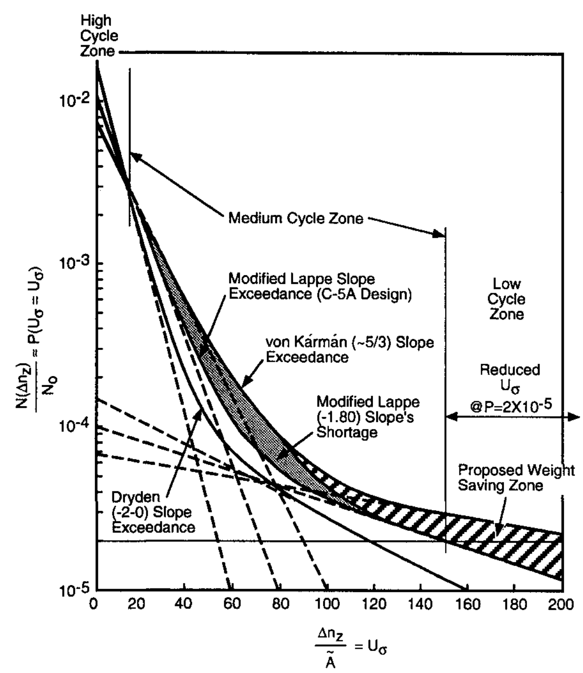

Fig. 3 One-segment mission analysis exceedance for a gust load critical aircraft.

Kármán spectrum ($D = 3$), and modified Lappe spectrum ($D = 2.5789$), is equally valid for any D.

Appendix A gives a lucid derivation of this claim. It proves hitherto suspected conservatism of the −5/3 slope von Kármán spectrum for all turbulence. Clearly it is only applicable for long continuous homogeneous turbulent patches. For severe, isolated turbulence, −1.8718 to −1.8071 slope is adequate. Incorporating this new slope for the storm (P_2 and

b_2) part of PSD method can lead to reduced airframe weight for a gust load critical aircraft. The actual weight reduction depends highly on how many high-frequency response modes are at this end. Figure 3 depicts a one-segment mission analysis' exceedance curve with both nonstorm and storm parts. It shows that the von Kármán spectrum overestimates the high load, low cycle end of the exceedance curve by its low N_0 and high $\Delta nz/\bar{A}$ values; if one remembers the expressions[22] for N_0, $\sigma^2_{\Delta nz}$, and $\bar{A}$:

$$N_0^2 = \int_0^\infty \omega^2 |H(j\omega)|^2 \Phi_{ww}(\omega)\, d\omega / 4\pi^2\sigma^2_{\Delta nz} \tag{12}$$

$$\sigma^2_{\Delta nz} = \int_0^\infty |H(j\omega)|^2 \Phi_{ww}(\omega)\, d\omega \tag{13}$$

$$\Delta nz/\bar{A} = (\Delta nz/\sigma_{\Delta nz})\sigma_{ww} = \eta_d \sigma_{ww} \tag{14}$$

where N_0 and $\Delta nz/\bar{A}$ are inversely and directly proportional to σ_{ww}. $|H(j\omega)|^2$ is the deterministic transfer function of Δnz, and Φ_{ww} is the input vertical gust velocity spectrum. The input PSD magnitudes at high frequency end ($\omega >> \omega_{\text{knee}}$) are proportional to $\omega^{-\alpha}$, hence, $\alpha = 2$, 1.80, and 5/3 are, respectively, the low, medium, and high spectra. Figure 4 shows this arrangement for a given turbulence scale factor L with $L/U_\infty = 1$ and $\sigma_{ww} = 1$.

Historical Sample and Lessons Learned

If both the nonstorm and storm part of the exceedance curve used the modified Lappe (-1.80 slope) spectrum,[9] the high and medium cycle end of the exceedance would be unconservative. If the actual nonstorm large patch continuous homogeneous turbulence behaves as the von Kármán spectrum, the former (modified Lappe) will predict fewer cycles than the latter (von Kármán); early high cycle fatigue of the airframe will result. It is probable that the Lockheed–Georgia Company's C-5A Galaxy's rewinging to reduce stress and increase service life to 30,000 flight hours[10] does reflect this trend. It was unavoidable to be a pioneer in PSD methods circa 1964–65, and to miss this difference.

Although Zbrozek[32] reported a measured -1.82 slope by Anne Burns in his paper, the impact of the reduced slope on gust response exceedance was fuzzy at best. Mandelbrot's findings for a $D = 2.5$–2.6 first appeared in 1974–76. Chorin reported his work that gives the correction to Kolmogorov exponents, $B = 0.17 \pm 0.03$ as late as 1981. The linking of $2.5 < D < 2.6$, $B = 0.17 \pm 0.03$ and $a \sim -1.80$ slope in this article (see Table 2, rows 4 and 5) is the only known derivation from basic principles to date; not from correctly processed measured gust velocity time histories.[33]

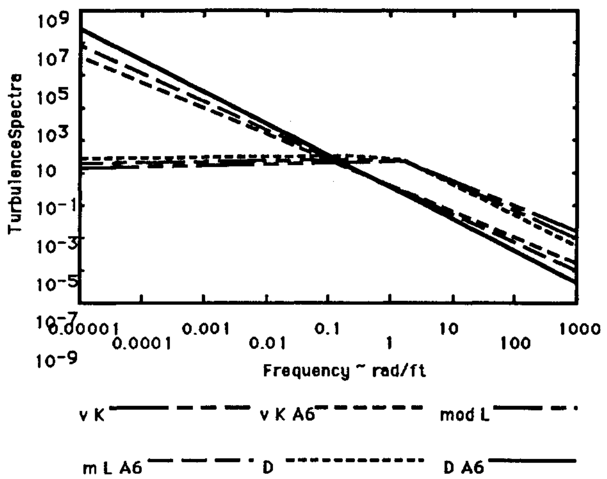

Fig. 4 Comparison of various turbulence spectra.

Proposed FAA Requirements Change

It is not 20/20 hindsight, but a belated reality check, to propose a near-term change of using von Kármán spectrum ($-5/3$ slope), P_1, b_1 for nonstorm part only, and modified Lappe (-1.80 slope), P_2, b_2 for storm part of the exceedance curve in FAR 25 requirements. Adopting this procedure, the future airframe designs will be more optimum than they are now, especially when the design life of the new aircraft such as Boeing 777, McDonnell Douglas MD-12, and Airbus Industrie's post A-330, 340, exceeds 50,000 flight hours, and the limit load exceedance level will be less than 2×10^{-5} as advocated by FAA today. Figure 3 illustrates this claim clearly.

It is true that the von Kármán spectrum is the least conservative at the very low load high cycle end (see Fig. 3), yet no known deficiency reports from L-1011, DC-10, Boeing 757, and 767 have surfaced throughout the years. The heuristic reason must be that the overestimated limit (and ultimate) loads at exceedance level 2×10^{-5} always cover at least the modified Lappe spectrum high cycle exceedance level. Thus, it seems reasonable in applying the proposed new mix: von Kármán ($-5/3$) slope, P_1, b_1 nonstorm and modified Lappe (-1.80) slope, P_2, b_2 storm method; an additional check to see that either the modified Lappe or at least the von Kármán slope high cycle exceedance is met by the new reduced (no longer overestimated) limit (and ultimate) loads.

Although the fractal dimensions derived spectra do not rule out with probability zero that a pathological mix of modified Lappe and von Kármán spectra can happen in one nonstorm patch of homogeneous continuous turbulence; the very requirement that $D_T < D \leq E$ from fractal geometry[7] will render $D = D_T = 2$ impossible and $D = E = 3$ improbable. This author predicts the highest realizable D will be at most 2.8928 (row 3 of Table 2). This gives a -1.7024 slope.

It is fortunate that Stewart[34] has shown that Langford's quasiperiodic strange attractor model for bifurcation theory matches the classic Taylor-Couette flow, which qualitatively resembles the Earth's rotation in still air, exactly. The topological surfaces for phase transition given in Figs. 128 and 129 of Ref. 34 verify the correctness of the third model of Table 2. Clearly, both quasiperiodic and chaotic surfaces are the same as row 3 of Table 2 with a radius $<<\infty$. Row 3 is the limiting case for a radius $\rightarrow \infty$.

With such strong evidence, a long-term change in reducing gust load critical airframe weight is readily achievable by reducing the von Kármán slope $-5/3$ to -1.69 with P_1 and b_1 for the nonstorm part of exceedance. However, it seems prudent not to incorporate this step for the near-term change. It will be less venturing after one verifies the modified Lappe slope -1.80, P_2, and b_2 storm exceedance first. The eventual long term change will come second as time goes on.

Realistic Assessments of SDG Method's Role in Gust Loads Determination

The present SDG method is inadequate as a gust loads design tool. First objections that attract one's attention are the very inefficient computational algorithm.[2] It is inconceivable any airframe manufacturer, large or small, will invest 20 times longer computer machine (CPU) time to obtain mere consistent $\bar{\gamma} = 10.4\bar{A}$ values that are low in comparison to the PSD method's $x_{\text{limit}} = U_\sigma \bar{A} = 25$–$150\bar{A}$.

The rationales that reject and accept the SDG method are the following:

1) Any gust response is a stochastic behavior of a deterministic system. The former is inherently stochastic (or random) due to the inputs (gust velocities), the latter is the airplane model that is a function of geometry and aerodynamics. If one neglects the measurable geometric and material imperfections, the system response is deterministic.

2) No amount of elegance in the input alone can diffuse a single degree-of-freedom (plunge) airplane model into a multi-degree-of-freedom model.

3) The only way to date in extracting the deterministic characteristics from the chaotic gust response are the PSD method that requires the conversion of both output/input time histories by fast Fourier transform (FFT) to PSD format first, and then process the output/input spectra by the well-known linear system approach [i.e., $|H(j\omega)|^2 = \Phi_{out}(\omega)/\Phi_{in}(\omega)$].

4) There is no known technique from the classical geometric toolbox by the addition of Mandelbrot's self-similar fractals as of 1983 to solve this aircraft design problem, although many useful characteristics of fractally homogeneous turbulence depend solely upon D (e.g., Taylor's homogeneous turbulence has $D = 3$, and $B = 0$, leaving the classic Kolmogorov exponent 2/3, and von Kármán $-5/3$ slope). All these findings describe the input turbulence more accurately, but not the output responses.

5) In all of Jones' work, non-PSD description of the input gust shape with its connection to turbulence dominates the scene. No concrete systematic methods leading to the results similar to design envelope analysis and/or mission analysis[22] are forthcoming.

6) The only substantial result is $\bar{\gamma} = 10.4\bar{A}$; however, the finding has quite limited utility as a design tool. $\bar{\gamma}_{max} = 25$–$42\bar{A}$ for x_{limit}, and 59–$150\bar{A}$ for $x_{ultimate}$ in practical aircraft design seem to be more realistic.

7) One usage derived by the SDG method that saves aircraft design cost and time, is the publication of a RAE and NASA jointly authorized compendium of $\bar{\gamma}$ values of response quantities for available aircraft types calculated by Jones and Perry III et al. The values, therein, could be invaluable for small and large airframe manufacturers alike to obtain, at least, some "in the ballpark" estimates of design gust loads in the following format:

$$x_{limit} = U_\sigma \bar{A} = U_\sigma \bar{\gamma}/10.4 \tag{15}$$

$$x_{ultimate} = U_{\sigma max}\bar{A} = U_{\sigma max}\bar{\gamma}/10.4 \tag{16}$$

where $U_\sigma = 25$–42 fps, and $U_{\sigma max} = 59$–150 fps.

A rational way to determine the U_σ and $U_{\sigma max}$ value is the following:

1) If one knows the design probability level and altitude, use Fig. 2b's U_σ vs $P(U_\sigma > u_\sigma)$ = constant and altitude.

2) If one knows the design aircraft speed and altitude, use Fig. 2a's U_σ vs V_C, V_D, or V_B and altitude.

Recommendations and Conclusions

The near-term recommendations are the following:

1) The FAA should change the FAR 25 requirements for continuous gust design criteria as follows: Use von Kármán spectrum with $-5/3$ slope for nonstorm part of the exceedance with its usual P_1 and b_1 value. Use modified Lappe spectrum with -1.80 slope for storm part of the exceedance with its usual P_2 and b_2 value. The provisional spectral shape[9] has the following expression:

$$\Phi_{ww}(\Omega) = 0.8L\sigma_{ww}^2/(1 + \Omega L)^{1.8} \tag{17}$$

where $\Omega = \omega/U_\infty$ is the reduced frequency in rad/s, U_∞ is the free airstream velocity, and L is the scale of turbulence. However, Eq. (17) will be subject to changes agreed upon by agencies responsible for FAR 25 and JAR 25. This article only requires the slope at $\omega \gg \omega_{knee}$ be -1.80. The incorporation of L and σ_{ww} into the equivalent of Eq. (17), and the subsequent reconciliation with the Fourier transforms of $|x|^\alpha$ per Eq. (A6) remains unsolved. Preliminary calculations with $L/U_\infty = 1$ and $\sigma_{ww} = 1$ for the new expression show a better fit to measured data without a knee at lower frequencies.[22] Figure 4 depicts some of the new trends.

2) An investigation of Eq. (A6) relationship to three-dimensional turbulence[35] is desirable. Greater weight reduction for low aspect ratio aircraft (e.g., Concorde, SST, NASP, and HSCT) could be sizable when the combined effects are quantified.

3) The VG, VGH data updates to cover newer airplanes' operations at higher altitudes are mandatory. The isoprobability lines' trends from 19,000 ft and up could lead to more realistic blends into the existing sea level to 70,000-ft isoprobability lines based on P_1, P_2 values from 0 to 70,000 ft in.[9] and VG, VGH data from 5000–19,000-ft piston engine operations[36] and B-66B low-altitude flights.[37]

4) SDG method's $\bar{\gamma} = 10.4\bar{A}$ must expand to include $\bar{\gamma}_D = C_D\bar{A}$ and $\bar{\gamma}_{ML} = C_{ML}\bar{A}$, where C_D and C_{ML} are values replacing 10.4 for new similarity parameters shown in Table 2. Preliminary analysis shows that $C_D = 5.47$ and $C_{ML} = 8.04$, or the same order of 10.4 to be of little utilitarian values; nevertheless, they are valuable as the expected pedantic end for mathematical completeness in the SDG method, and an important verification of which expression ($k = 1/D$, $D - 2/3$, or $5 - D/6$; given $D < 3$) for k, the similarity parameter, is better for gust load analysis.

The long-term recommendations are the following:

1) Besides 1 above, replace the $-5/3$ von Kármán slope by -1.69 to -1.70 for the nonstorm part of the exceedance. Reduce the -1.80 slope for modified Lappe further to -1.84 to -1.87 if near-term usage of -1.80 for the storm part of the exceedance finds no known deficiency.

2) Governments and/or airframe manufacturers should encourage basic research in fractal geometry and chaos-related mathematical subjects that could advance gust response studies. The payback from one breakthrough could be enormous. The switch from the deterministic 1-cosine-shaped gust method to the current PSD method exemplifies this observation.

The conclusions from this article are as follows:

1) The PSD method is an acceptable way of performing gust load analysis. Insofar as improvements to the method; changing slopes from $-5/3$ von Kármán value to -1.80 for storm and -1.69 for nonstorm is a positive start in designing an efficient gust load critical aircraft. Reduction in airframe weight is always a goal that all manufacturers want, if the reasons are justifiable by new findings.

2) This article has, in principle, removed the 10-yr-old lament from Mandelbrot's epilog.[7] "The geometric face of this theory of scaling grew in importance, and gave size to fractal geometry. Given the strong geometric flavor of the early studies of turbulence and of critical phenomena, one may have expected a theory of fractals [for turbulence] to develop in either of these contexts. But none developed." If one recalls that the classic Kolmogorov and Burgers turbulence models are the benchmark in fluid mechanics, one will agree, at least in spirit, this claim.

3) The present SDG method should not be ostracized as a resurrected ramp-hold gust method. It is useful in raising the consciousness of this author, and hopefully other researchers, to the henceforth unfamiliar subject of fractal geometry.

4) The established ad hoc international committee and its organizer(s) should actively seek increased communication between themselves and the researchers in industries and schools. No timely dissemination of a SDG method before 1983 in the public domain did inadvertently cast the method into an "untried, mysterious" mood that it does not deserve.

Appendix A: Derivation of Turbulent Velocity Spectrum

Mandelbrot's variance of turbulent velocity[7] definition gives the following expression:

$$\langle |V(x) - V(x + r)|^2 \rangle = |r|^{2/3+B} \tag{A1}$$

By expanding the squared expression, and applying the expectation term by term

$$\langle |V(x) - V(x + r)|^2 \rangle = \langle V^2(x) \rangle - 2\langle V(x)V(x + r) \rangle + \langle V^2(x + r) \rangle \tag{A2}$$

Rearranging terms from Eq. (A2), the autocorrelation function for $V(x)$ becomes

$$\langle V(x)V(x + r)\rangle = -|r|^{2/3+B} + \langle V^2(x)\rangle + \langle V^2(x + r)\rangle/2 \tag{A3}$$

Assuming homogeneity, $\langle V^2(x)\rangle = \langle V^2(x + r)\rangle = \sigma_{VV}^2 =$ const, or

$$\langle V(x)V(x + r)\rangle = -|r|^{2/3+B}/2 + \sigma_{VV}^2 \tag{A4}$$

Applying Lighthill's[8] Fourier transform for $|x|^\alpha$, Eq. (A4) becomes the turbulent velocity spectrum:

$$\Phi_{VV}(\omega) = \frac{1}{2}\pi\int_{-\infty}^{\infty}\langle V(x)V(x + r)\rangle e^{-j\omega r}\,\mathrm{d}r = \sigma_{VV}^2/\pi j\omega - \left\{\frac{1}{2}\pi\cos\pi\Big/2\left(\frac{5}{3} + B\right)\right\}\left(\frac{2}{3} + B\right)!(2\pi|\omega|)^{-(5/3+B)} \tag{A5}$$

Taking the limit $j\omega \rightarrow \infty$, or $\omega^2 \rightarrow \infty$, the $\omega >> \omega_{\mathrm{knee}}$ part of the spectrum becomes

$$\underset{j\omega\rightarrow\infty}{L}\ \Phi_{VV}(\omega) = -\{\tfrac{1}{2}\pi\cos\pi/2(\tfrac{5}{3} + B)\}(\tfrac{2}{3} + B)!(2\pi|\omega|)^{-(5/3+B)} \propto \omega^{-(5/3+B)} \tag{A6}$$

This expression completes the derivation.

Acknowledgments

The author would like to thank Steve I. P. Chen for his computer support, and Allied-Signal Aerospace, Aerospace Systems and Equipment, for permission to publish this article. The ideas advanced herein were seeded many years ago at Lockheed–Georgia Co., and rekindled recently by the works of Jones and Perry III et al.

References

[1]Jones, J. G., "A Unified Procedure for Meeting Power-Spectral-Density and Statistical-Discrete-Gust Requirement for Flight in Turbulence," AIAA Paper 86-1011, May 1986.

[2]Perry, B., III, Pototzky, A. S., and Woods, J. A., "NASA Investigation of a Claimed 'Overlap' Between Two Gust Response Analysis Methods," *Journal of Aircraft*, Vol. 27, No. 7, 1990, pp. 605–611.

[3]Jones, J. G., "An Equivalence Between Deterministic and Probabilistic Design Criteria for Linear Systems," *Journal of Sound and Vibration*, Vol. 125, No. 2, 1988, pp. 341–356.

[4]Jones, J. G., "Statistical-Discrete-Gust Method for Predicting Aircraft Loads and Dynamic Response," *Journal of Aircraft*, Vol. 26, No. 4, 1989, pp. 382–392.

[5]Hentschel, H. G. E., and Procaccia, I., "Fractal Nature of Turbulence as Manifested in Turbulent Diffusion," *Physical Review A (Rapid Communication)*, Vol. 27, No. 2, 1983, pp. 1266–1269.

[6]Yamazaki, H., "Breakage Models: Lognormality and Intermittency," *Journal of Fluid Mechanics*, Vol. 219, Oct. 1990, pp. 181–193.

[7]Mandelbrot, B. B., *The Fractal Geometry of Nature*, W. H. Freeman, San Francisco, CA, 1983, pp. 97–108, 277–279, 422–424, Chaps. 10, 11, 30, and 42.

[8]Lighthill, M. J., *Introduction to Fourier Analysis and Generalised Functions*, Cambridge Univ. Press, Cambridge, England, UK, 1962, pp. 30–45.

[9]Firebaugh, J. M., "Evaluations of a Spectral Gust Model Using VGH and VG Flight Data," *Journal of Aircraft*, Vol. 4, No. 6, 1967, pp. 518–525.

[10]Taylor, J. W. R., *Jane's All the World's Aircraft 1978–1979*, Jane's Yearbooks, London, Oct. 1978, pp. 370, 371.

[11]Chen, R. P., Yokota, F. T., Allen, D. V., and Friedericy, J. A., "Production Acceptance Testing Using an Improved Acoustic Signature Analysis," National Aerospace Engineering and Manufacturing Meeting, Society of Automotive Engineers Paper 730929, Los Angeles, CA, Oct. 1973.

[12]Jones, J. G., Forster, G. W., and Earwicker, P. G., "Wavelet Analysis of Gust Structure in Measured Atmospheric Turbulence Data," *Journal of Aircraft*, Vol. 30, No. 1, 1993, pp. 94–99.

[13]Chen, R. P., and Bernard, M. C., "Nonstationary Random Pulses Representation of Ground Roughness for Taxiing Aircraft," *Journal of Aircraft*, Vol. 13, No. 11, 1976, pp. 911–918.

[14]Perry, B., III, Pototzky, A. S., and Woods-Vedeler, J. A., "Reply by the Authors to Bernard Etkin," *Journal of Aircraft*, Vol. 29, No. 4, 1992, p. 743.

[15]Etkin, B., "Comment on "NASA Investigation of a Claimed 'Overlap' Between Two Gust Response Analysis Methods,"" *Journal of Aircraft*, Vol. 29, No. 4, 1992, pp. 741, 742.

[16]Tucker, H. G., *An Introduction to Probability and Mathematical Statistics*, Academic Press, New York, 1962, pp. 81–94.

[17]Houbolt, J. C., "Interpretation and Design Application of Power Spectral Gust Response Analysis Results," *Proceedings of the AIAA/ASME 7th Structures and Materials Conference* (Cocoa Beach, FL), AIAA, New York, 1966, pp. 77–85.

[18]Houbolt, J. C., "Atmospheric Turbulence," *AIAA Journal*, Vol. 11, No. 4, 1973, pp. 421–437.

[19]Anon., *Federal Airworthiness Regulations, Part 25, Airworthiness Standards: Transportation Category Airplanes*, Federal Aviation Administration, Washington, DC, 1988.

[20]Wang, J. C. T., and Shen, S. F., "Rational New Approach to the Response of an Aircraft Entering Atmospheric Turbulence," *AIAA Journal*, Vol. 18, No. 2, 1980, pp. 129–137.

[21]Etkin, B., "Turbulent Wind and Its Effect on Flight," *Journal of Aircraft*, Vol. 18, No. 5, 1981, pp. 327–345.

[22]Hoblit, F. M., *Gust Loads on Aircraft: Concepts and Applications*, AIAA, New York, 1988. pp. 21–81, 187–202, Chaps. 4, 5, 12 and 13.

[23]Parzen, E., *Modern Probability Theory and Its Applications*, Wiley, New York, 1964, pp. 226–228.

[24]Lin, Y. K., "Probability Distributions of Stress Peaks in Linear and Nonlinear Structures," *AIAA Journal*, Vol. 1, No. 5, 1963, pp. 1133–1138.

[25]Chen, W.-Y., "Application of Rice's Exceedance Statistics to Atmospheric Turbulence," *AIAA Journal*, Vol. 10, No. 8, 1972, pp. 1103–1105.

[26]Cramèr, H., *Mathematical Methods of Statistics*, Princeton Univ. Press, Princeton, NJ, 1963, pp. 182–185.

[27]Press, H., and Steiner, R., "An Approach to the Problem of Estimating Severe and Repeated Gust Loads for Missile Operations," NACA TN 4332, Sept. 1958.

[28]Gumbel, E. J., "Statistical Theory of Extreme Values and Some Practical Applications," *National Bureau of Standards, Applied Mathematics Series 33*, Feb. 1954.

[29]Press, H., "The Application of the Statistical Theory of Extreme Values to Gust Loads Problems," NACA Rept. 991, 1950.

[30]Rucker, R., *Mind Tools, The Five Levels of Mathematical Reality*, Houghton Mifflin, Boston, MA, 1987, pp. 161–177.

[31]Peitgen, H. O., and Saupe, D., *The Science of Fractal Images*, Springer–Verlag, New York, 1988, pp. 65, 91.

[32]Zbrozek, J. K., "Atmospheric Gusts, Present State of the Art and Further Research," *Journal of the Royal Aeronautical Society*, Vol. 69, Jan. 1965, pp. 27–45.

[33]Eichenbaum, F. D., "The Application of Matrix Methods to Clear Air Turbulence Measurement," AIAA Paper 66-967, Nov.–Dec. 1966.

[34]Stewart, I., *Does God Play Dice? The Mathematics of Chaos*, Blackwell, Cambridge, MA, 1989, pp. 303–320.

[35]Eichenbaum, F. D., "A General Theory of Aircraft Response to Three-Dimensional Turbulence," *Journal of Aircraft*, Vol. 8, No. 5, 1971, pp. 353–360.

[36]Walker, W. G., and Copp, M. R., "Summary of VGH and VG Data Obtained from Piston Engine Transport Airplanes from 1947 to 1958," NASA TN D-29, Sept. 1959.

[37]Saunders, K. D., "B-66B Low Level Gust Study," *Technical Analysis*, Vol. I, Wright Air Development Division, WADD TR-60-305, March 1961.